

Structures of Fibrous Supramolecular Assemblies Constructed by Amino Acid Surfactants: Investigation by AFM, SANS, and SAXS

Toyoko Imae,^{*,†,1} Naoki Hayashi,[†] Takayoshi Matsumoto,[‡] Toshio Tada,[‡] and Michihiro Furusaka[§]

^{*}Research Center for Materials Science and [†]Graduate School of Science, Nagoya University, Nagoya 464-8602, Japan; [‡]Division of Material Chemistry, Faculty of Engineering, Kyoto University, Kyoto 606-8317, Japan; and [§]Institute of Materials Structure Science, High Energy Accelerator Research Organization, Tsukuba 305-0801, Japan

Received March 22, 1999; accepted February 3, 2000

Aqueous gel-like solutions of *N*-acyl-L-aspartic acids ($C_n\text{Asp}$, $n = 14, 16, 18$) and *N*-dodecanoyl- β -alanine ($C_{12}\text{Ala}$) were prepared at pH 5–6 at room temperature. Structures of supramolecular assemblies in the solutions were investigated by atomic force microscopy (AFM), small-angle neutron scattering (SANS), and small-angle X-ray scattering (SAXS). The cross-sectional radii, 22–30 Å, of helical, fibrous assemblies were obtained from analysis of SANS for 1% gel-like $C_n\text{Asp}$ solutions. Three Bragg spacings were observed in a SANS spectrum for a 6% $C_{16}\text{Asp}$ solution. $C_n\text{Asp}$ molecules are associated into the unit chain of a helical bilayer strand with a diameter of 50–60 Å. Unit chains where linear bilayers twist form a double strand with helical sense of $\sim 650\text{-}\text{\AA}$ pitch. It was confirmed from AFM images that cylindrical fibers in a gel-like $C_{12}\text{Ala}$ solution had a circular cross-section. The SAXS spectrum showed characteristic Bragg spacings. Cylindrical $C_{12}\text{Ala}$ fibers consist of multilamellar layers of period $\sim 34\text{-}\text{\AA}$. The fibers are laterally organized with period 365–380 Å. © 2000 Academic Press

Key Words: helical fiber; cylindrical fiber; supramolecular assembly; gel; amino acid surfactant; *N*-acyl-L-aspartic acid; *N*-dodecanoyl- β -alanine; atomic force microscopy; small-angle neutron scattering; small-angle X-ray scattering.

INTRODUCTION

Rodlike micelles are one of the linear supramolecular assemblies, and their structures and solution properties have been intensively investigated. These kinds of assembly are constructed by the noncovalent self-organization of small molecules, the motive force of which is hydrophobic interaction between long alkyl chains. Fibrous chains are another kind of linearly extended assembly, which is constructed in gel-like solutions of amphiphiles (1–16) and nonamphiphiles (17–21). Especially, assemblies with helical sense are characteristic of chiral component molecules. Such a character is seen in amphiphilic molecules with hydrophilic head groups such as amino acids, nucleosides, and sugars.

Rich and Blow (2) have studied X-ray diffraction of sodium deoxycholate mixed with glycylglycine. They suggest the for-

mation of the helical complex in a gel-like solution. Tachibana *et al.* (4) have reported the transmission electron microscopic (TEM) observation of 12-hydroxystearate fibers and confirmed the relation of helical sense to optical activity. Hidaka *et al.* (5) have revealed that the driving force for the formation of fibrous assemblies is hydrogen bonding. Nakashima *et al.* (6) have studied the time dependence of fiber formation by dark-field optical microscopy. Fuhrhop *et al.* (7) have reported that NMR spectra of *N*-alkylaldonamides display a temperature-dependent phase equilibrium between micelles and fibers. Yanagawa *et al.* (9) have observed a characteristic Cotton effect for fibers of 5'-phosphatidyl nucleoside derivatives. The Cotton effect is similar to that for polynucleotides, indicating the similarity of structures. Terech (8) has investigated small-angle neutron scattering (SANS) and small-angle X-ray scattering (SAXS) for organogels of 12-hydroxystearate derivatives and discussed their molecular arrangement in fibers. Hanabusa *et al.* (11) have reported the gelling of organic liquids by small molecular gelling agents. The gel is built up through intermolecular hydrogen bonding between amphiphiles. Shimizu *et al.* (13) have discovered a unique self-assembly of vesicle-enclosing tubular organic fibers. Amyloid-like filaments have been discovered by Yamada *et al.* (15). Their secondary structure is a pseudoparallel β -sheet. The formation of thick filaments in solutions of fluoroalkyl amphiphiles has been investigated by Imae *et al.* (14) and Emmanouil *et al.* (16).

Single-chain amphiphiles with amino acid head groups, which are known as gelation materials, form fibrous molecular assemblies in aqueous solutions and display characteristic rheological behavior (10, 12). *N*-Acyl-L-aspartic acids ($C_n\text{Asp}$, $n = 14, 16, 18$, $C_{n-1}\text{H}_{2n-1}\text{CONHCH}(\text{COOH})\text{CH}_2\text{COOH}$) construct helical fibers when vesicular solutions at pH 5–6 are cooled below the Krafft temperature. *N*-Dodecanoyl- β -alanine ($C_{12}\text{Ala}$, $C_{11}\text{H}_{23}\text{CONHCH}_2\text{CH}_2\text{COOH}$) molecules are associated into cylindrical fibers at pH below 6 at room temperature. The mechanism of gelation for amphiphiles with amino acid head groups should be related to the molecular arrangement in fibers, besides the morphological structure of fibers and the interaction with solvent. In our previous work (10, 12), speculative models of molecular organization in helical $C_n\text{Asp}$ fibers

¹ To whom correspondence should be addressed.

were proposed. However, the fine structure in cylindrical C_{12} Ala fibers was not inferred, although the comparison of the construction of nonhelical C_{12} Ala fibers with that of helical C_n Asp fibers is important in clarifying the role of molecular chirality to the helical sense.

In this paper, we examined fibrous assemblies of amino acid surfactants, C_n Asp and C_{12} Ala, by using atomic force microscopy (AFM), small-angle neutron scattering (SANS), and small-angle X-ray scattering (SAXS). We discussed the structure of fibrous chains and the molecular arrangement in fibers. SANS and SAXS are beneficial methods for studying organization on the molecular scale, the aim of this work.

EXPERIMENTAL

C_n Asp and C_{12} Ala, which were supplied by Mitsubishi Petrochemical Co., Ltd., are the same samples previously used (10, 12). Standardized NaOH and HCl solutions are commercial products. Water was redistilled from alkaline $KMnO_4$ and boiled for 1 h. A solvent, D_2O (99.75% purity), for SANS measurements was purchased from Wako Pure Chemical Industries, Ltd.

Gel-like solutions were prepared as follows: solids were dissolved in water at high temperature (60–80°C) and solutions were adjusted to pH 5–6. The solutions were initially transparent, but they became opalescent after being maintained at high

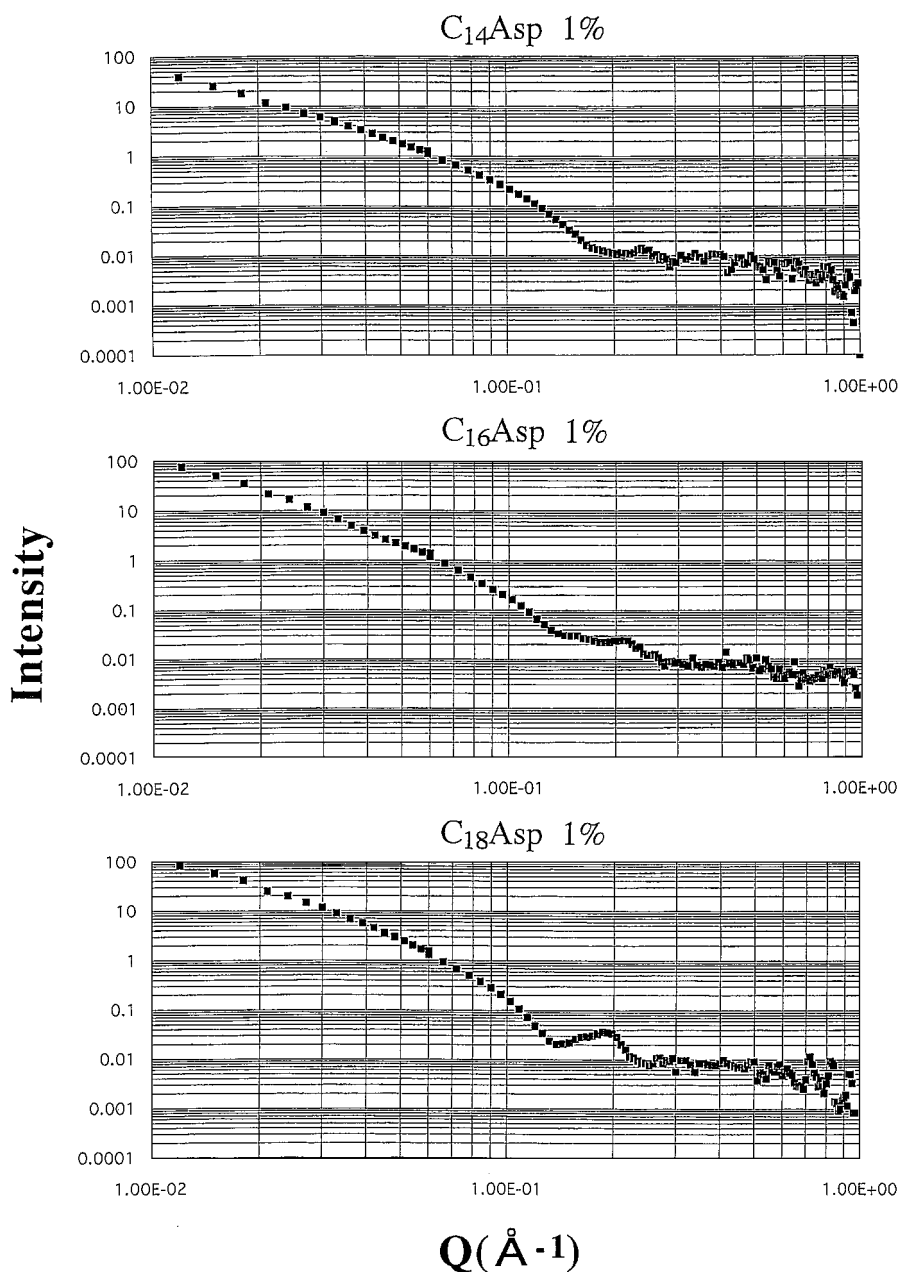


FIG. 1. SANS data for gel-like 1% C_n Asp solutions.

temperature for more than 2–3 h. When the opalescent solutions were cooled to a lower temperature (room temperature), the solutions became gel-like.

AFM observation was carried out with a Nanoscope III apparatus produced by Digital Instruments Co., Ltd. The specimens for the observation were prepared by dropping and drying a small amount of solution on a mica substrate. Therefore, it is a xerogel and not a genuine gel with the solvent. Measurements were carried out with the tapping mode at room temperature.

SANS measurements were performed at room temperature on a WINK small/medium-angle diffractometer at the High Energy Accelerator Research Organization. The instrument can cover a wide momentum transfer range ($Q = 0.01\text{--}15 \text{ \AA}^{-1}$) by utilizing a very wide incident neutron wavelength range ($\lambda = 1\text{--}16 \text{ \AA}$). The beam size at the sample position was $20 \times 20 \text{ mm}^2$. SAXS was measured by a 6-m point focusing SAXS camera at the High Intensity X-ray Laboratory in Kyoto University. The wavelength of the X ray was 1.542 \AA (CuK α radiation). Measurements were carried out at 25°C .

RESULTS AND DISCUSSION

$C_n\text{Asp}$ Fibers

SANS intensities $I(Q)$ for gel-like 1% $C_n\text{Asp}$ solutions are shown as double-logarithmic plots against momentum transfer Q in Fig. 1, where $Q = (4\pi/\lambda)\sin(\theta/2)$ and θ is the scattering angle. Intensities gradually decreased with increasing Q at lower Q values. In addition, small peaks were observed at around $Q = 0.2 \text{ \AA}^{-1}$. Those peaks shifted toward lower Q with increasing alkyl chain lengths.

The scattering intensity for the local structure of rod particles is described by

$$I(Q)Q = \pi n_p (V^2/L)(\rho - \rho_s)^2 \exp(-R_{G,C}^2 Q^2/2), \quad [1]$$

for the range $QL \gg 1$ and $QR_{G,C} \ll 1$, where n_p is the number density of colloidal particles and V and L are the volume and length of the rod, respectively. ρ and ρ_s are the mean coherent scattering length density of the particles and that of the solvent, respectively. $R_{G,C}$ is the radius of gyration for the cross-section of the rod and is related to the cross-sectional radius R_t by the equation

$$R_{G,C} = R_t/\sqrt{2}. \quad [2]$$

Supposing that fibrous $C_n\text{Asp}$ assemblies have rod structures, Eq. [1] can be applied. When the logarithm of $I(Q)Q$ was plotted as a function of Q^2 , there was a linear part at the Q range corresponding to $Q^2 = 0.005\text{--}0.02 \text{ \AA}^{-2}$. Deviations from the straight line at lower Q^2 values are contributions from the informations at longer distances such as the whole size of the fiber or a characteristic fiber segment length. Deviations at higher Q^2 values suffer shorter distance contributions such as surface structure.

Using Eqs. [1] and [2], radii of gyration and radii of cross-section were evaluated from the linear parts of the Guinier plots.

TABLE 1
Structural Parameters for Molecular Assemblies in Aqueous 1% $C_n\text{Asp}$ Solutions

n	$R_{G,C}$ (\AA)	R_t (\AA)	R_{cal} (\AA)
14	15.9	22.4	22.5
16	19.2	27.2	25.0
18	21.5	30.4	27.5

The calculated values are listed in Table 1. R_{cal} in Table 1 is the calculated molecular length of amphiphiles with the trans-zigzag hydrocarbon chain configuration. The cross-sectional radii are close to the calculated molecular lengths, suggesting that unit chains have radii of the molecular length. It should be noticed that the upper limit of the Q value calculated by $2\pi/R_t$ satisfies the Guinier region described previously.

If a small peak around $Q = 0.2 \text{ \AA}^{-1}$ is interpreted as a Bragg peak from a cross-sectional size, the distance calculated from the equation $R = 2\pi/Q_{\text{max}}$ must be consistent with the radius evaluated from the Guinier plot. However, this was not the case. Then, a small peak around $Q = 0.2 \text{ \AA}^{-1}$ must be the first peak of the first-order Bessel function for intraparticle structure function (22). Calculation usually shows such a first peak around 0.2 \AA^{-1} . Since the fiber thickness of $C_n\text{Asp}$ is fairly monodisperse or homogeneous (10), the first peak can be observed.

Two kinds of models were proposed for $C_n\text{Asp}$ fibers in our previous work (10). One model consists of a planar bilayer sheet which has a rectangular cross-section with a shorter side of $60\text{--}65 \text{ \AA}$. In another model, $C_n\text{Asp}$ fibers are constructed from helical bilayer strand units where the linear bilayer with almost double thickness of molecular length twists. The helical strands form a double-strand structure. Figure 2 illustrates the schematic representation of such a model. SANS results support the latter

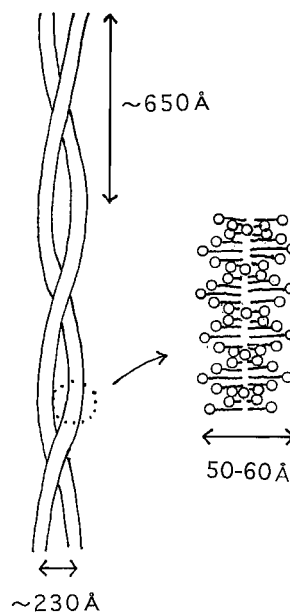


FIG. 2. Schematic representation of a possible model for $C_n\text{Asp}$ fibers.

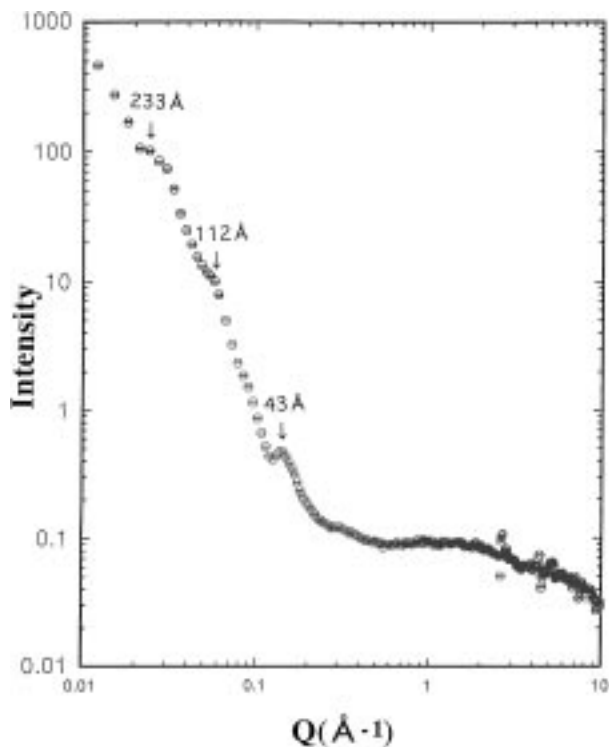


FIG. 3. SANS data for a gel-like 6% $C_{16}Asp$ solution.

model (Fig. 2), that is, a helical bilayer strand of unit chains with a cross-sectional radius of molecular length, because a unit chain with a molecular length radius is not adequate for the former sheet model.

SANS results for an aqueous 6% $C_{16}Asp$ solution are given in Fig. 3. Three Bragg peaks were observed; they corresponded to the spacings $R = 43, 112,$ and 233 \AA , which were calculated from Bragg peaks Q_{\max} along with the equation $R = 2\pi/Q_{\max}$. Those peaks do not appear in dilute solutions. The formation of helical, fibrous assemblies in 1% C_nAsp solutions has been confirmed in cryo-TEM photographs (10). The minimum and maximum widths of the cross-section are ~ 120 and $\sim 200 \text{ \AA}$, respectively, and the helical pitch of the fibers is $\sim 650 \text{ \AA}$. Fibers are partly associated by lateral interaction. The spacing of $\sim 230 \text{ \AA}$ obtained from a SANS experiment may be assigned to the repeating distance between the parallel orderings of fibers. Then the $\sim 110\text{-\AA}$ spacing will correspond to the second order of $\sim 230\text{-\AA}$ spacing. The 43-\AA spacing may be the higher order of $\sim 230\text{-\AA}$ spacing or the helical pitch of the unit chain. The alternative possibility is that the Bragg peaks observed may be higher order reflections of the helical pitch of a helical bilayer strand. Then, measurement of much lower Q values is desirable.

$C_{12}Ala$ Fibers

Figure 4 shows an AFM photograph for a dried specimen, i.e., a xerogel prepared from a gel-like 2% $C_{12}Ala$ solution.

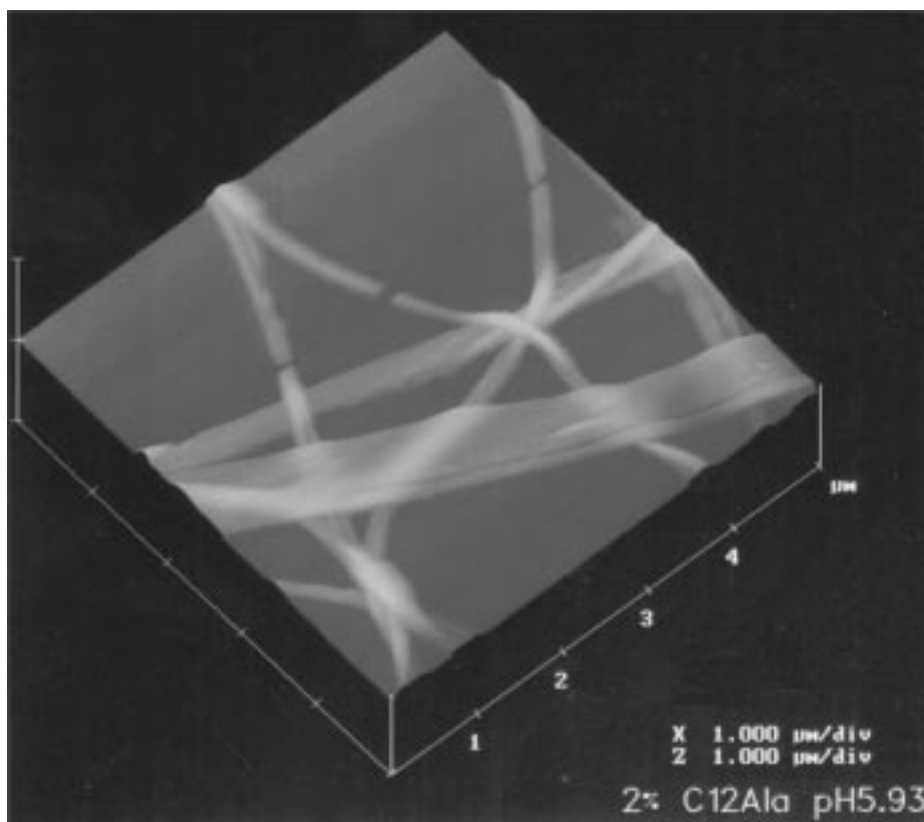


FIG. 4. An AFM image (stereic figure) of a dried specimen, i.e., a xerogel of $C_{12}Ala$ fibers prepared from a 2% solution.

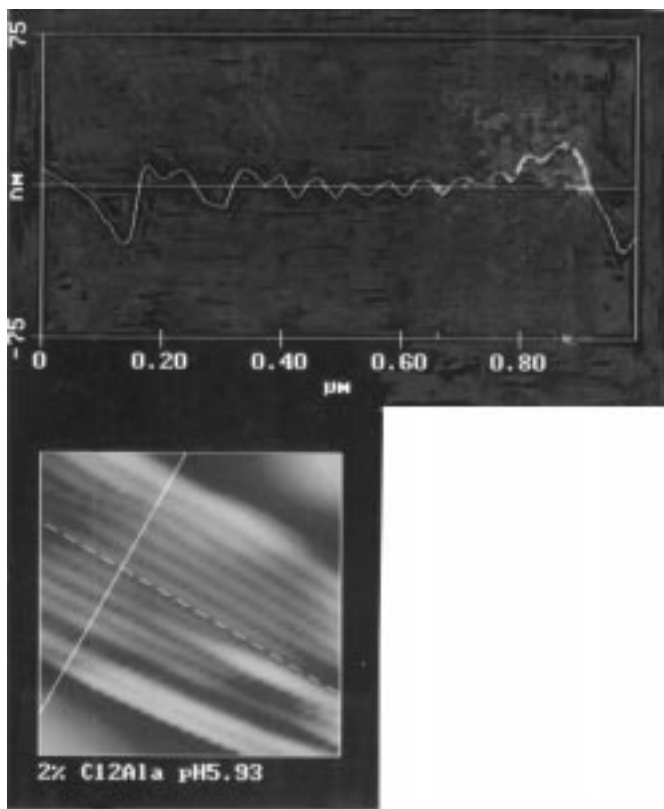


FIG. 5. Section analysis of a part of Fig. 4.

Cylindrical fibers with a constant width formed bundles or ribbons. Figure 5 gives a cross-sectional analysis of the ribbon. The fibers had almost equivalent heights and widths (400–430 Å), indicating that their cross-section is circular. Such three-dimensional information was not obtained from cryo-TEM (10), although the width, ~ 400 Å, of the cross-section was visible in the TEM. The repeating distances between fibers were ~ 50 Å wider than those observed by TEM. Lateral interaction between fibers in water is maintained by hydrogen bonding (10). When the specimen is dried in air, such interaction is weakened, resulting in wider distances between fibers.

Figure 6 shows plots of SAXS results for aqueous C_{12} Ala solutions at different concentrations. There were some Bragg peaks. The numerical values of the main spacings are listed in Table 2. Spacings corresponding to 34- to 35- and 365- to 380-Å spacings were observed at all concentrations, indicating that those peaks are intrinsic to the fiber structure. The spac-

TABLE 2
Bragg Spacings Measured for Aqueous C_{12} Ala Solutions

Concentration	Spacings R in Å		
0.4	34.2		380
1	34.7		380
2	34.1		365
3	34.4	38.5	365
4	33.9	38.5	365

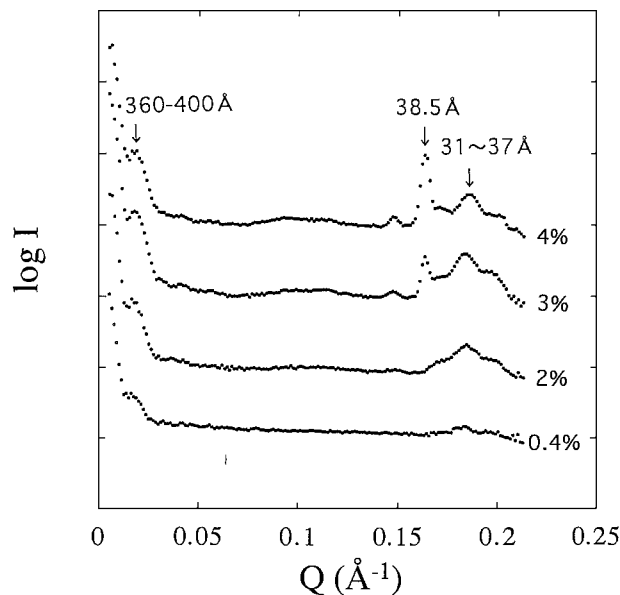


FIG. 6. SAXS data for gel-like C_{12} Ala solutions at different concentrations.

ings decreased with increasing C_{12} Ala concentration. A strong peak at 365–380 Å is assigned to the lateral repeating distance of cylindrical fibers, being consistent with that observed in the microscopy. The spacings of 34–35 Å is close to twofold the calculated molecular length of C_{12} Ala, corresponding to the thickness of the bilayer unit, that is, the lamellar layer, although the higher order spacings were not observed. The intensity of a peak at 38.5 Å increased remarkably with increasing concentration. Therefore, this may be the repeating distance of bilayers in the crystalline state, indicating crystallization of bundles or ribbons as well as the junction region in a polymer gel.

A schematic model for C_{12} Ala fibers is represented in Fig. 7. Fibers interact laterally with an interfiber distance of ~ 400 Å. Each fiber consists of cylindrical multilamellar layers with a repeating distance of ~ 34 Å. The decrease in both distances with increasing concentrations implies the shortening of water layers.

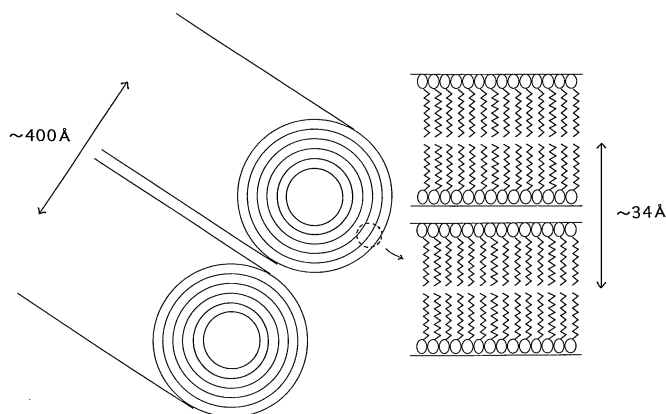


FIG. 7. Schematic representation of a possible model for C_{12} Ala fibers.

CONCLUSIONS

It is assumed that the construction of helical assemblies goes through processes starting from two kinds of unit arrangements. Those unit chains are the helical bilayer strand (7) and the planar bilayer sheet (6). Gel-like solutions of amphiphilic molecules with amino acid head groups were investigated by microscopic observation and scattering examination in the present work. C_n Asp molecules formed helical fibers. It was proved from the SANS experiment that the unit arrangement was the helical bilayer strand but not the planar bilayer sheet. The unit strands formed a double strand. The helical sense of C_n Asp fibers results from the existence of asymmetric carbon.

C_{12} Ala molecules were associated into cylindrical fibers, which were reported to be formed by racemic amphiphilic molecules (4, 6, 7). The AFM and SAXS investigations demonstrated that cylindrical fibers of C_{12} Ala had a circular cross section with multilamellar layers. This suggests that the fibers constructed from C_{12} Ala molecules without asymmetric carbon are different, in the molecular arrangement, from chiral C_n Asp fibers.

The formation of bilayer units by C_n Asp and C_{12} Ala molecules in the fiber is induced and stimulated by the hydrogen bonding between amide groups themselves and between carboxylate and carboxyl groups, which coexist at pH near the pK (10). The importance of hydrogen bonding in the formation of helical fibers was already suggested (5). The hydrogen bonding between carboxylate and carboxyl groups also occurs between fibers, resulting in lateral interaction between fibers and the network structure. It was reported for the thermoplastic elastomer of polybutadiene derivative that the hydrogen bonding between side chains formed thermoreversible networks and changed the rheological property with temperature (23).

Terech (8) has investigated organogels of 12-D-hydroxystearic acid derivatives by utilizing SANS and SAXS. He concluded that the cross-sectional shape is either a monodisperse square or an elongated rectangle, depending on the solvent and the concentration. The models for fibers of 12-D-hydroxystearic acid derivatives are different from those for C_n Asp and C_{12} Ala fibers in the present work.

ACKNOWLEDGMENT

This work was supported in part by Grant-in-Aid 05403012 for Scientific Research from the Ministry of Education in Japan.

REFERENCES

- Hotten, B. W., and Birdsall, D. H., *J. Colloid Interface Sci.* **7**, 284 (1952).
- Rich, A., and Blow, D. M., *Nature* **182**, 423 (1958).
- Ramanathan, N., Currie, A. L., and Colvin, J. R., *Nature* **190**, 779 (1961).
- Tachibana, T., and Kambara, H., *J. Am. Chem. Soc.* **87**, 3015 (1965); Tachibana, T., Kitagawa, S., and Takeno, H., *Bull. Chem. Soc. Jpn.* **43**, 2418 (1970).
- Hidaka, H., Murata, M., and Onai, T., *J. Chem. Soc. Chem. Commun.* 562 (1984).
- Nakashima, N., Asakuma, S., Kim, J.-M., and Kunitake, T., *Chem. Lett.*, 1709 (1984); Nakashima, N., Asakuma, S., and Kunitake, T., *J. Am. Chem. Soc.* **107**, 509 (1985).
- Fuhrhop, J.-H., Schnieder, P., Rosenberg, J., and Boekema, E., *J. Am. Chem. Soc.* **109**, 3387 (1987); Fuhrhop, J.-H., Schnieder, P., Boekema, E., and Helfrich, W., *J. Am. Chem. Soc.* **110**, 2867 (1988); Fuhrhop, J.-H., Svenson, S., Boettcher, C., Rossler, E., and Vieth, H.-M., *J. Am. Chem. Soc.* **112**, 4307 (1990).
- Terech, P., and Wade, R. H., *J. Colloid Interface Sci.* **125**, 542 (1988); Terech, P., *Colloid Polym. Sci.* **269**, 490 (1991); *J. Phys. II France* **2**, 2181 (1992).
- Yanagawa, H., Ogawa, Y., Furuta, H., and Tsuno, K., *Chem. Lett.* 269 (1988); *J. Am. Chem. Soc.* **111**, 4567 (1989).
- Imae, T., Takahashi, Y., and Muramatsu, H., *J. Am. Chem. Soc.* **114**, 3414 (1992).
- Hanabusa, K., Tange, J., Taguchi, Y., Koyama, T., and Shirai, H., *J. Chem. Soc. Chem. Commun.* 390 (1993); Hanabusa, K., Matsumoto, Y., Miki, T., Koyama, T., and Shirai, H., *J. Chem. Soc. Chem. Commun.* 1401 (1994).
- Imae, T., and Kidoaki, S., *J. Jpn. Oil Chem. Soc.* **44**, 301 (1995).
- Shimizu, T., Kogiso, M., and Masuda, M., *Nature* **383**, 487 (1996); *J. Am. Chem. Soc.* **119**, 6209 (1997); Shimizu, T., and Masuda, M., *J. Am. Chem. Soc.* **119**, 2812 (1997).
- Imae, T., Krafft, M.-P., Giulieri, F., Matsumoto, T., and Tada, T., *Prog. Colloid Polym. Sci.* **106**, 52 (1997).
- Yamada, N., Ariga, K., Naito, M., Matsubara, K., and Koyama, E., *J. Am. Chem. Soc.* **120**, 12192 (1998).
- Emmanouil, V., El Ghoul, M., André-Barrès, C., Guidetti, B., Rico-Lattes, I., and Lattes, A., *Langmuir* **14**, 5389 (1998).
- Lehn, J.-M., Mascal, M., DeCian, A., and Fischer, J., *J. Chem. Soc. Chem. Commun.* 479 (1990).
- Ghadiri, M. R., Granja, J. R., Milligan, R. A., Mcrec, D. E., and Khazanovich, N., *Nature* **366**, 324 (1993).
- Jokić, M., Makarević, J., and Žinić, M., *J. Chem. Soc. Chem. Commun.* 1723 (1995).
- Imae, T., Gagel, L., Tunich, C., Platz, G., Iwamoto, T., and Funayama, K., *Langmuir* **14**, 2197 (1998).
- Imae, T., Ikeda, Y., Iida, M., Koine, N., and Kaizaki, S., *Langmuir* **14**, 5631 (1998).
- Funayama, K., and Imae, T., *J. Phys. Chem. Solids* **60**, 1355 (1999).
- Stadler, R., and Freitas, L., *Colloid Polym. Sci.* **264**, 773 (1986); Freitas, L., and Stadler, R., *Macromolecules* **20**, 2478 (1987).